Iranian Journal of Chemical Engineering
Vol. 8, No. 4 (Autumn), 2011, IAChE

Use of Agricultural Waste for Removal of Cr(VI) from Aqueous Solution

I. Khazaei[1], M. Aliabadi[1], H. T. Hamed Mosavian[2]*
1- Young Researcher Club, Birjand Branch, Islamic Azad University, Birjand, Iran
2- Department of Chemical Engineering, Ferdowsi University of Mashhad, Mashhad, Iran

Abstract
Adsorption capacity of Cr(VI) onto activated carbon, almond and apricot shells was investigated in a batch system by considering the effects of various parameters like contact time, initial concentration, pH , temperature, agitation speed, absorbent dose and particle size.
The adsorption was solution pH dependent and the maximum adsorption was observed at solution pH of 2.0. The amounts of Cr(VI) adsorbed increased with increase in dose of both adsorbents and their contact time. A contact time of 30 min was found to be optimum. Experimental results show low cost biosorbent was effective for the removal of pollutants from aqueous solution. The pseudo-second-order kinetic model gave a better fit of the experimental data compared to the pseudo-first-order kinetic model. Experimental data showed a good fit with the Freundlich isotherm model.

Keywords: *Removal of Chromium, Adsorption Isotherm, Low Cost Absorbent, Kinetic*

1. Introduction
Heavy metals such as chromium, copper, lead, and cadmium in wastewater are hazardous to the environment.
Because of their toxicity, their pollution effect on our ecosystem presents a possible human health risk [1].
In recent years, increasing awareness of water pollution and its far reaching effects has prompted concerted efforts towards pollution abatement.
Among the different heavy metals, chromium is a common and very toxic pollutant introduced into natural waters from a variety of industrial wastewaters [2].
Chromium exists in either +3 or +6 oxidation states, as all other oxidation states are not stable in aqueous systems. Chromium (VI) is 100-1000 times more toxic to organisms than Cr(III) and more readily transported in soils[3].
The main industrial sources of chromium pollution are leather tanning, electroplating, metal processing, wood preservatives, paint and pigments, textile, dyeing, steel fabrication and canning industry [4].

* Corresponding author: Imane_khazaei@yahoo.com

Strong exposure of Cr(VI) causes cancer in the digestive tract and lungs and may cause epigastric pain, nausea, vomiting, severe diarrhoea, and hemorrhage. It is therefore, essential to remove Cr(VI) from wastewater before disposal[5]. The allowable limit of hexavalent chromium for the discharge to surface water is 0.1 mg/L[6].

In order to reduce Cr(VI) in these effluents to the standard level, an efficient and low cost method needs to be developed. The various methods of removal of Cr(VI) from industrial wastewater include filtration, chemical precipitation, adsorption, electrodeposition and membrane systems, or even ion exchange process. Chemical precipitation and reduction process needs other separation techniques for the treatment and disposal of high quantities of waste metal residual sludge produced. These techniques use various treatment chemicals and the residual Cr(VI) concentration required in the treated wastewater is not achieved because of the structure of the precipitates. The application of membrane systems for the wastewater treatment has major problems like membrane scaling, fouling and blocking. The drawback of the ion exchange process is the high cost of the resin, while the electrodeposition method is more energy intensive than other methods. Among these methods adsorption is one of the most economically favourable, as well as being a technically easy method[7].

Considerable attention has been devoted to the study of removal of heavy metal ions from solution by adsorption using agricultural materials such as waste wool, nut wastes, tree bark, modified cotton and sawdust [8–16]. Many agricultural byproducts such as almond and apricot shells are low-cost (or of no economic value) materials.

In this study, activated carbon, almond and apricot shells as adsorbent for Cr(VI) were used to determine adsorption efficiency as a function of contact time**,** initial concentration, absorbent dose, particle size, pH, temperature, agitation speed and constants of the adsorption isotherm.

2. Materials

Almond and apricot shells were prepared from agricultural solid wastes as adsorbents (major agricultural wastes of Birjand, Iran). Samples were washed several times with deionized water and dried (sun or mechanical). The adsorbents were then ground in a blender and stored for further use. Potassium dichromate and other chemicals were used of analytical reagent grade and were obtained from standard sources.

Activated carbon, Potassium dichromate and other chemicals were obtained from standard sources.

The physical properties of activated carbon have been listed in Table 1.

Table 1. Physical properties of activated carbon*

Activated carbon	Property
0.50–2.36	Particle size (mm)
900–1100	Surface area ($m^2\ g^{-1}$)
0.48	Solid density ($g\ cm^{-3}$)
0.53	Packing density ($g\ cm^{-3}$)
0.73	Pore volume ($ml\ g^{-1}$)

* Activated carbon type PHO 8/35 LBD

3. Method

A known weight (e.g. 2.0 g of absorbent) was equilibrated with 100 ml of the chromium solution of known concentration in a 250 ml glass flask at room temperature (25±1°C). Chromium solution was prepared by dissolving the potassium dichromate ($K_2Cr_2O_7$) in distilled water. Fresh dilutions were used for each study.

The pH of Chromium solution was adjusted with a 0.1M HCl/0.1M NaOH solution. Time of each experiment was kept at 30 min. These flasks were shaken on the shaker at 400 rpm. The samples were filtered through filter paper. The concentration of the samples was analyzed in a spectrophotometer (JENWAY 6305 UV/Vis model) using 1,5-diphenylcarbazide as the complexing agent at a wave length of 540 nm [17].

The Cr(VI) loadings on sorbents were computed based on mass balance through loss of metal from aqueous solution. Effect of various pH; temperature; dose 1, 2, 3, 4 and 6 g/100 ml of solution; contact time 5, 10, 15, 30, 40 min; initial concentration 0.5,1,2,4,5 ppm; particle size mesh>30, mesh<30, mesh>20; and agitation speed 50, 100, 300, 400, 700 rpm were studied. The adsorption capacity and intensity were calculated by the Langmuir, Freundlich and Temkin isotherm. In order to analyze the sorption rate, the kinetic data were modeled using Lagergren pseudo-first-order and pseudo-second order.

4. Results and discussion

4-1. Effect of contact time

Fig. 1 shows the adsorption of Cr(VI) by almond shell, apricot shell and activated carbon as a function of time. Initial Cr(VI) concentration 5 mg/l and absorbents dose of 2 g/100ml were used. Fig. 1 shows rapid adsorption in the initial 15 min for all biosorbent. Basically, the removal of Cr(VI) is rapid, but it gradually decreases with time until it reaches equilibrium. The necessary time to reach this equilibrium is about 15 min. Further increase in contact time did not show an increase in biosorption.

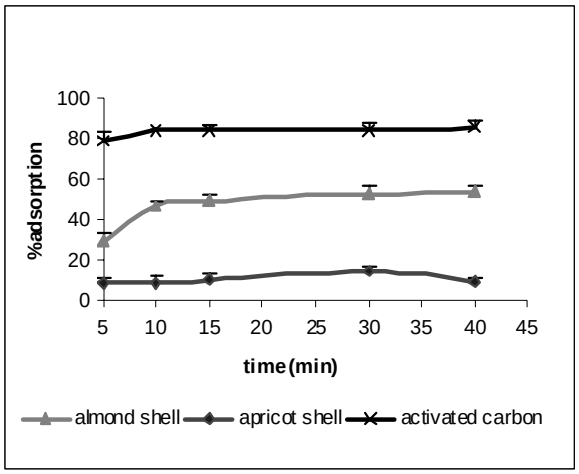

Figure 1. Effect of contact time on the removal of Cr(VI) (initial Cr(VI) concentration=5 mg/l, adsorbent dose=2 g/100 ml, temperature=26 ºC, agitation speed= 400 rpm)

4-2. Effect of initial Cr (VI) concentration

The effect of Cr(VI) concentration on the sorbent by varying the initial Cr(VI) concentration (0.5, 1, 2, 4 and 5 mg/l) for a 30 min time interval has been shown in Fig. 2.

The percentage removal was decreased with increase in Cr(VI) concentration. At low concentrations the ratio of available surface to the initial Cr(VI) concentration is larger, so the removal becomes independent of initial concentrations. However, in the case of higher concentrations this ratio is low; the

percentage removal then depends upon the initial concentration. From the results, it is revealed that within a certain range of initial metal concentration, the percentage of metal adsorption on absorbent is determined by the sorption capacity of the absorbent.

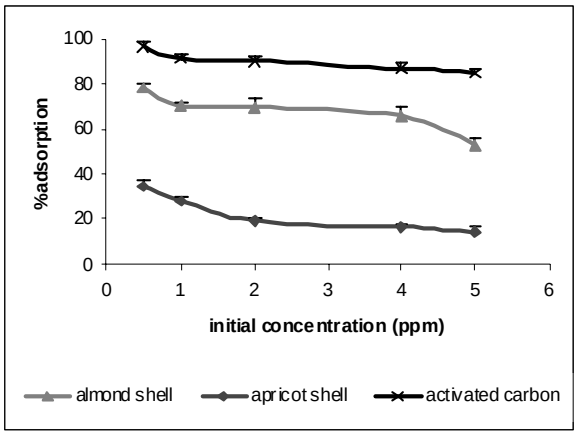

Figure 2. Effect of initial Cr (VI) concentration on the removal of Cr(VI) (adsorbent dose=2 g/100 ml, temperature=26 ºC, agitation speed= 400 rpm, contact time=30 min)

4-3. Effect of absorbent dose

The effect of adsorbent dose on Cr (VI) uptake was investigated by varying the adsorbent dose (1, 2, 3, 4 and 6 g/100 ml) for a time interval of 30 min (Fig. 3). Experimental results showed that the percentage removal Cr (VI) increases with the increasing amount of adsorbent up to 3 g for activated carbon. After this dose of adsorbent no significant change was observed, but for almond and apricot shells percentage removal Cr(VI) increases with the increasing amount of adsorbent .

The phenomenon of increase in percent chromium removal with increase in adsorbent dose was due to the availability of more and more adsorbent surfaces for the solutes to adsorb. However, very slow increase in removal beyond an optimum dose may be attributed to the attainment of equilibrium between adsorbate and adsorbent at the operating conditions. This effect has been termed "solid concentration effect" i.e. overcrowding of particles, by Mehrotra et al. [15].

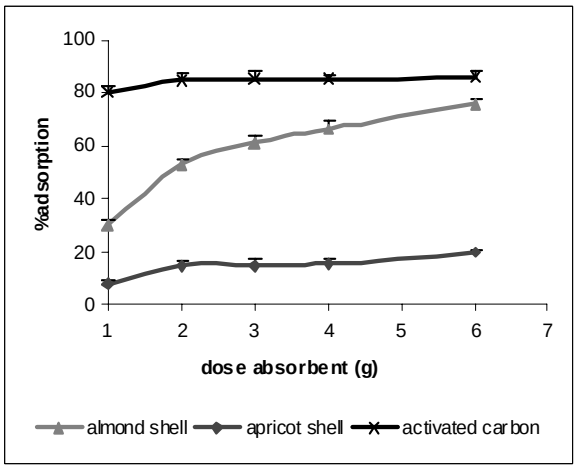

Figure 3. Effect of amount of adsorbent on the removal of Cr(VI) (initial Cr(VI) concentration=5 mg/l, temperature=26ºC, agitation speed= 400 rpm, contact time=30 min)

4-4. Effect of pH

The pH of the aqueous solution is an important controlling parameter in the adsorption process. As shown by the results, adsorption of Cr (VI) was higher at lower pH and decreased with increasing pH (Fig. 4). Also shown in the results, the optimum initial pH was observed at pH 2.0.

The dominant chromium compound within the solution at pH=2 is $HCr\,O_4^-$ ($Cr\,O_4^{-2}$) and also, $Cr_2O_7^{-2}$ exists. Removal of Cr(III) at pH=2 is zero whereas its removal percentage is very high at pH=5; however, removal percentage of Cr(VI) is significantly low. This shows that the pH of the solution is a very important parameter for the removal of

Cr(VI), which is the toxic form of the chromium metal. At pH=2, due to the excess amount of H^+ ions within the medium, the active site on the absorbent positively charged. This causes a strong attraction between these sites and negatively charged $HCrO_4^-$ ions;

$$OH_2^+ + HCrO_4^- \leftrightarrow OH_2^+(HCrO_4^-) \qquad (1)$$

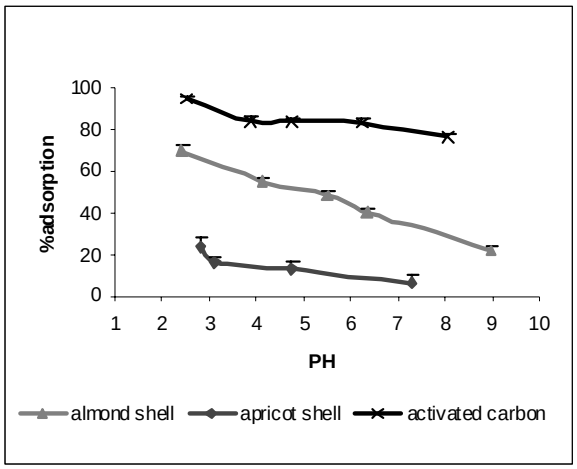

Figure 4. Effect of pH on the removal of Cr(VI) (initial Cr(VI) concentration=5 mg/l, temperature=26 ºC, adsorbent dose=2 g/100 ml, agitation speed= 400 rpm, contact time=30 min)

At low pH values active sites are positively charged. Therefore, negative metals adsorption increases significantly. When pH value increases, the surface of the adsorbent becomes neutral and a decrease in the adsorption is observed. When adsorbent surface is negatively charged, adsorption decreases significantly. This behavior is specific for the chromium ions and is different for the divalent metals. Chromium ions release hydroxide ions to the solution instead of protons [14].

4-5. Effect of temperature

Adsorption is considered as an exothermic process; therefore it is expected that the equilibrium concentration increases (i.e. amount of adsorbed material decreases) with increasing temperature. But some chemical adsorption processes are endothermic processes; therefore, increase in temperature leads to increase in both adsorption rate and amount of adsorbed materials. Since this trend was observed in this study, adsorption of Cr(VI) is possibly a chemical adsorption process.

The adsorption of Cr(VI) at different temperatures shows an increase in the adsorption capacity when the temperature is increased (Fig. 5). Similar trends are observed for all the other concentrations. This indicates that the adsorption reaction is endothermic in nature. The enhancement in the adsorption capacity may be due to the chemical interaction between adsorbates and adsorbent, creation of some new adsorption sites or the increased rate of intraparticle diffusion of Cr(VI) ions into the pores of the adsorbent at higher temperatures.

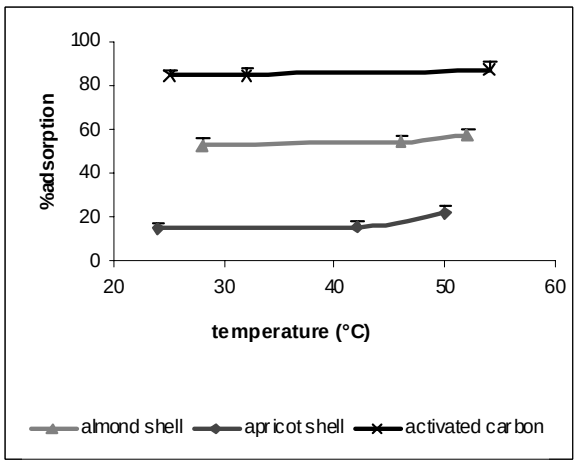

Figure 5. Effect of temperature on the removal of Cr(VI) (initial Cr(VI) concentration=5 mg/l, adsorbent dose=2 g/100ml, agitation speed= 400 rpm, contact time=30 min)

Kinetic energies of chromium ions were low at low temperatures. Therefore, it is a very difficult and time-consuming process for ions to reach the active sites on the adsorbent. Increase in temperature causes an increase in the mobility of the ions. If the temperature is further increased, the kinetic energies of chromium ions become higher than the potential attractive forces between active sites and ions.

The standard Gibb's energy was evaluated by

$$\Delta G^0 = -RT \ln K_C \quad (2)$$

The equilibrium constant 1 K_c was evaluated at each temperature using the following relationship

$$K_C = \frac{C_{Ae}}{C_e} \quad (3)$$

Where C_{Ae} is the amount adsorbed on solid at equilibrium and C_e is the equilibrium concentration.

The other thermodynamic parameters such as change in standard enthalpy (ΔH^o) and standard entropy (ΔS^o) were determined using the following equations

$$\ln K_C = \frac{\Delta S^0}{R} - \frac{\Delta H^0}{RT} \quad (4)$$

ΔH^o and ΔS^o were obtained from the slope and intercept of the Van't Hoff's plot of ln$K$c versus 1/T as shown in Fig. 6.

Positive value of ΔH^o indicates that the adsorption process is endothermic. The negative values of ΔG^o reflect the feasibility of the process and the values become more negative with the increase in temperature. Standard entropy determines the disorderliness of the adsorption at solid–liquid interface.

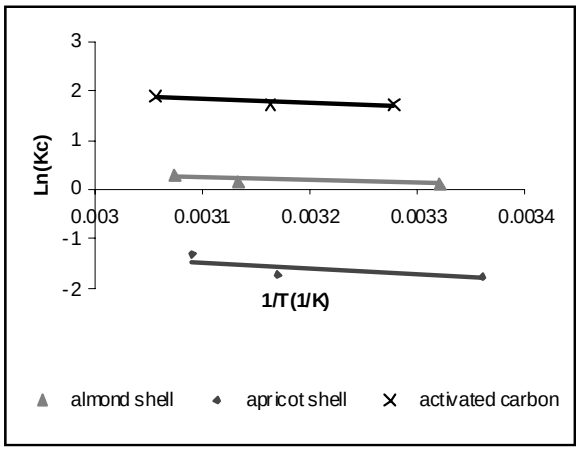

Figure 6. Vant Hoff's plot at ambient temperature

4-6. Effect of particle size

The effect of particle size on the Cr(VI) adsorption capacity of almond shell, apricot shell and activated carbon has been shown in Fig.7.

It is evident from Fig.7 that the particle size of sorbents has a significant effect on Cr(VI) sorption. The larger sorbent size showed lesser Cr(VI) removal as compared to the smaller sorbent size. The reason may be that the surface area available for adsorption decreases with the increase of particle size for the same dose of sorbent, providing less active surface sites for adsorption of sorbate. The reduction in Cr(VI) removal capacity with the increase in sorbent size gives an idea about the porosity of sorbent i.e., if the sorbent is highly porous then it would have no significant effect on Cr(VI) removal at equilibrium.

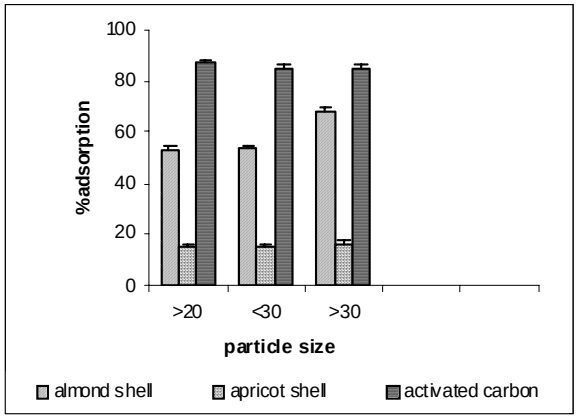

Figure 7. Effect of particle size on the removal of Cr(VI) (initial Cr(VI) concentration=5 mg/l, temperature=26 ºC, adsorbent dose=2 g/100 ml, agitation speed= 400 rpm, contact time=30 min)

4-7. Effect of agitation speed

Biosorption studies were carried out with a magnetic shaker at ambient temperature. The agitation speed varied from 50 to 700 rpm. The biosorption rate increased because of the increasing kinetic energy of the Cr(VI) particles (Fig. 8).

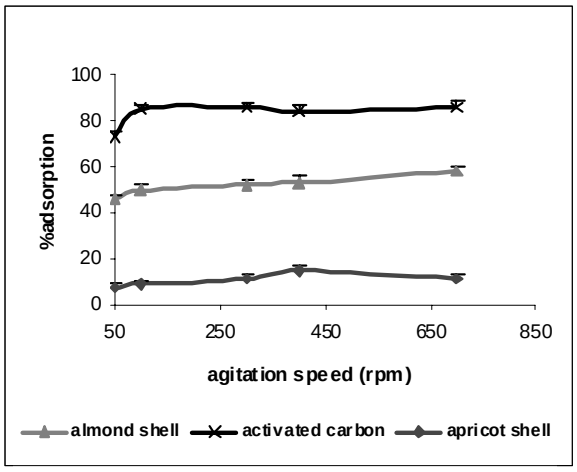

Figure 8. Effect of agitation speed on the removal of Cr(VI) (initial Cr(VI) concentration=5 mg/l, Temperature=26 ºC, adsorbent dose=2 g/100 ml, contact time=30 min)

Basically, the removal of Cr(VI) is rapid, but it gradually decreases with increased agitation speed, and the percent of removal of Cr(VI) of the solutions did not change after 400 rpm, therefore, Cr(VI) adsorption efficiency was maximal at 400 rpm.

4-8. Adsorption isotherm

Adsorption equilibrium data were fitted to the Langmuir, Freundlich and Temkin isotherms. Langmuir isotherm is based on the monolayer adsorption of chromium ions on the surface of absorbent sites and is expressed in the linear form as [13]

$$\frac{Ce}{x/m} = \frac{1}{KV_m} + \frac{Ce}{V_m} \tag{5}$$

Where Ce is the equilibrium solution concentration, x/m the amount adsorbed per unit mass of adsorbent, m the mass of the adsorbent, V_m the monolayer capacity, and K is equilibrium constant related to the heat of adsorption by equation:

$$K = K_0 \times \exp(\frac{q}{RT}) \tag{6}$$

Where q is the heat of adsorption.

Freundlich isotherm describes the heterogeneous surface energies by multilayer adsorption and is expressed in linear form as [13]

$$Log\frac{x}{m} = LogK_f + \frac{1}{n}LogCe \tag{7}$$

Where K_f and $1/n$ are Freundlich constants related to adsorption capacity and intensity of adsorption, and other parameters are the same as in the Langmuir isotherm. The term $\log(x/m)$ can be plotted against $\log Ce$ with slope $1/n$ and intercept $\log K_f$.

Temkin isotherm, based on the heat of adsorption of the ions, which is due to the adsorbate and adsorbent interactions taken in linear form, is given by [4].

$$\frac{x}{m} = (\frac{RT}{b})LnA + (\frac{RT}{b})LnCe$$
$$\frac{RT}{b} = B \quad (8)$$

Where b is the Temkin constant related to heat of sorption (J/mol), A the Temkin isotherm constant (L/g), R the gas constant (8.314 J/(mol K)) and T is the absolute temperature (K).

The theoretical parameters of isotherms along with regression coefficient have been listed in Table 2.

The three isotherms are compared with each other in Figs. 9, 10 and 11.

The results indicate that the Freundlich equation fits the experimental data better than the Langmuir and Temkin equations.

4-9. Adsorption kinetics modeling

To find the potential rate-controlling steps involved in the process of biosorption of Cr(VI) onto almond shell, apricot shell and activated carbon, both pseudo first-order and pseudo second-order kinetic models have been used to fit the experimental data.

4-9-1. Pseudo-first-order model

The pseudo-first-order kinetic model was described by Lagergren [18];

$$\frac{d_q}{d_t} = k_1(q_e - q_t) \quad (9)$$

Table 2. Isotherm constants for various adsorption isotherms

Adsorbent name	Langmuir constants		
	V_m $(mg.g^{-1})$	K $(L.mg^{-1})$	R^2
Apricot shell	0.0536	0.484	0.934
Almond shell	0.210	0.846	0.924
Activated carbon	0.310	2.470	0.886
Freundlich constants			
	$1/n$	K_f $(mg.g^{-1})$	R^2
Apricot shell	0.55	0.016	0.990
Almond shell	0.680	0.089	0.969
Activated carbon	0.611	0.240	0.987
Temkin constants			
	B	$A(L.g^{-1})$	R^2
Apricot shell	0.011	5.488	0.941
Almond shell	0.042	11.129	0.927
Activated carbon	0.051	48.594	0.885

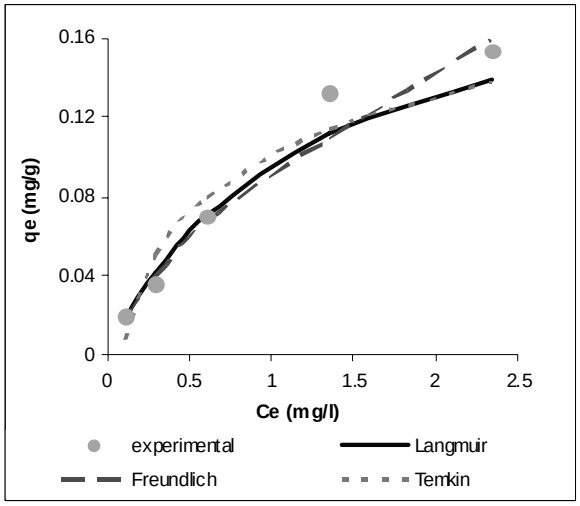

Figure 9. Equilibrium isotherms of Cr (VI) onto almond shell

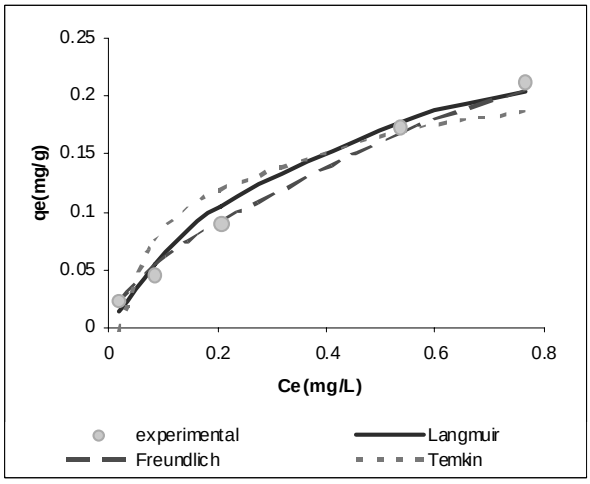

Figure 10. Equilibrium isotherms of Cr (VI) onto activated carbon

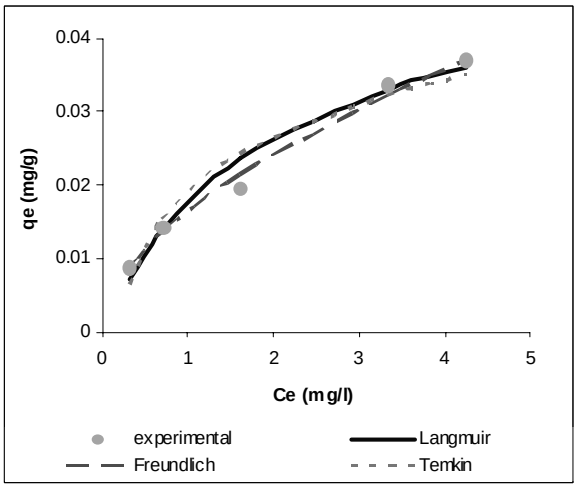

Figure 11. Equilibrium isotherms of Cr (VI) onto apricot shell

Where q_e (mg g^{-1}) and qt (mg g^{-1}) are the amounts of the Cr(VI) adsorbed on the adsorbent at equilibrium and at time t, respectively; and k_1 (min^{-1}) is the rate constant of the first order model. After integration and applying boundary conditions q_t=0 at t=0 and q_t=q_t at t=t, the integrated form of Eq. 9 becomes:

$$\ln(q_e - q_t) = \ln q_e - k_1 t \tag{10}$$

A straight line of ln(qe−qt) versus t suggests the applicability of this kinetic model; q_e and k_1 can be determined from the intercept and slope of the plot, respectively.

It is important to note that the experimental q_e must be known for the application of this model. Table 3 shows the pseudo-first-order constants, q_e and k_1, along with the corresponding correlation coefficients for initial Cr(VI) concentration of 5 ppm. The calculated q_{ecal} value was not in good agreement with the experimental value of q_{eexp}. These observations suggested that the pseudo-first-order model is not suitable for modeling the adsorption of Cr(VI) onto almond shell, apricot shell and activated carbon.

4-9-2. Pseudo-second-order model

The pseudo-second-order model is based on the assumption that the rate-limiting step is chemical sorption or chemisorption involving valance forces through sharing or exchange of electrons between sorbent and sorbate as covalent forces [19, 20]. The model has the following form [21]:

$$\frac{dq}{dt} = k_2(q_e - q_t)^2 \tag{11}$$

Table 3. Calculated kinetic parameters for pseudo first-order and second-order kinetic models for the adsorption of Cr(VI)

$C_\circ$ (mg L^{-1})	$q_{e\ exp}$ (mg g^{-1})	Pseudo-first-order			Pseudo-second-order			Adsorbent name
		$q_{e\ cal}$ (mg g^{-1})	k_1 (min^{-1})	R^2	$q_{e\ cal}$ (mg g^{-1})	k_2 (g $mg^{-1}min^{-1}$)	R^2	
5	0.133	0.122	0.176	0.933	0.149	1.826	0.997	Almond shell
5	0.037	0.018	0.031	0.750	0.028	47.588	0.892	Apricot shell
5	0.212	0.042	0.264	0.930	0.226	4.691	0.998	Activated carbon

Where k_2 (g mg^{-1} min^{-1}) is the rate constant of the second-order equation; q_e (mg g^{-1}) is the maximum adsorption capacity; q_t(mg g^{-1}) is the amount of adsorbed at time t (min).

After definite integration by applying the boundary conditions qt=0 at t=0 and qt=qt at t=t, the Eq. 11 takes the form presented in equation 12:

$$\frac{t}{q_t} = \frac{1}{k_2 q_e^2} + \frac{t}{q_e} \qquad (12)$$

If second-order kinetics is applicable, the plot of t/qt against t shows a straight line; q_e and k_2 can then be obtained from the slope and intercept of the plot, respectively. For the initial Cr(VI) concentration of 5 ppm, k_2 and $qe_{\ cal}$ values, along with the corresponding correlation coefficients have been presented in Table 3. The correlation coefficient was nearly equal to unity and calculated $q_{e\ cal}$ value was very close to the experimental value of $q_{e\ exp}$. The results indicated that the pseudo-second-order adsorption mechanism is predominant for the adsorption of Cr(VI) onto almond shell, apricot shell and activated carbon, and it is considered that the rate of the Cr(VI) adsorption process is controlled by the chemisorption process.

4-10. Fourier transform infrared analysis (FT-IR)

The FT-IR spectra of almond and apricot shells before and after adsorption of chromium have been shown in Figs. 12-15. The spectra of adsorbents were measured within the range of 500–4000 cm−1 wave number. For the FT-IR study, 5 mg of finely ground biomass was encapsulated in 400 mg of KBr in order to prepare the translucent sample disks.

The FTIR spectra obtained revealed that there were various functional groups detected on the surface adsorbents before and after adsorption. Table 4 presents the fundamental peaks of the adsorbents before and after use. There are some peaks that were shifted, disappeared and new peaks were also detected.

As seen in Table 4, these band shifts indicated that it was the bonded –OH groups and aliphatic C–H groups in particular which played a major role in chromium (VI) biosorption on almond shell.

Table 4. Some fundamental frequencies of the studied adsorbents (before and after use)

Band positions (cm^{-1})					Adsorbent
Bending vibrations	**OCH3**	**C=O**	**C–H**	**O–H**	
610.1	1054.9	1743.5	2925.2	3400.0	Almond shell native
893.0, 609.6	1054.7	1743.1	2924.9	3394.4	Almond shell-Cr(VI)
555.7	1042.2	1742.7	2916.8	3357.8	Apricot shell native
607.7	1051.8	1742.7	2925.3	3403.2	Apricot shell-Cr(VI)

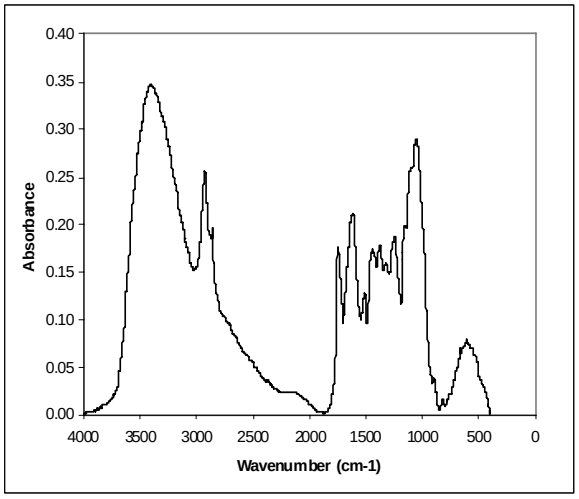

Figure 12. The FT-IR spectra of almond shell before adsorption

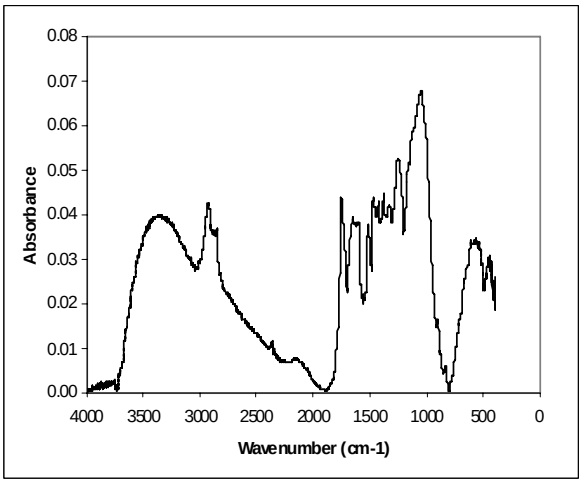

Figure 14. The FT-IR spectra of apricot shell before adsorption

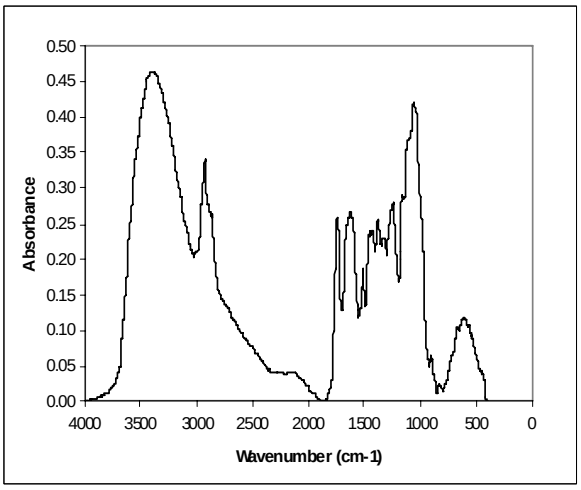

Figure 13. The FT-IR spectra of almond after adsorption

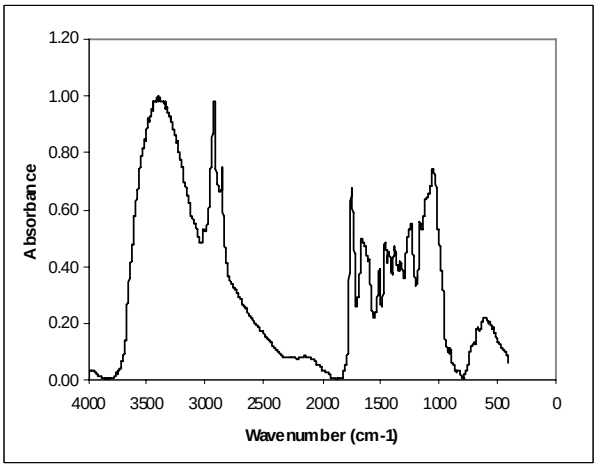

Figure 15. The FT-IR spectra of apricot after adsorption

5. Conclusions

The following conclusions are made based on the results of the present study and scientific information derived from literature:

1. The present investigation shows that the almond and apricot shells are effective and inexpensive biosorbents for the removal of Cr(VI) from aqueous solutions.
2. The removal of Cr(VI) from aqueous solutions strongly depends on the contact time, initial concentration, pH, temperature, agitation speed, absorbent dose and particle size.
3. The amounts of Cr(VI) adsorbed increased with an increase in dose of both adsorbents and their contact time. A contact time of 30 min was found to be optimum.
4. The percentage removal of Cr(VI) increased with increasing temperature. The maximum adsorption capacity was obtained at solution pH of 2.0.
5. The Langmuir, Freundlich and Temkin adsorption models used to represent the experimental data fitted very well to the Freundlich isotherm model.
6. The kinetics of Cr(VI) adsorption onto almond shell, apricot shell and activated carbon followed the pseudo-second-order model.

References

[1] Nourbakhsh, M., Sag, Y., Ozar, D., Aksu, Z. and Kutsal, C., "A comparative study of various biosorbents for removal of chromium (VI) ions from industrial waste waters," Process Biochem., 29 (1), (1994)1–5.

[2] Donmez, D. and Aksu, Z., "Removal of chromium(VI) from saline wastewaters by Dunaliella species," Process Biochem., 38 (5), (2002)751–762.

[3] Karthikeyan, T., Rajgopal, S. and Miranda, L. R.,"Chromium (VI) adsorption from aqueous solution by Hevea Brasilinesis sawdust activated carbon," J. Hazard. Mater., B124 (2005) 192-199.

[4] Raji, C. and Anirudhan, T.S., "Chromium (VI) adsorption by sawdust: kinetics and equilibrium," Indian J. Chem. Technol., 4, (1997) 228–236.

[5] Namila, D. and Mungoor, A., "Dye adsorption by a new low cost material Congo red-1," Indian J. Environ., 13, (1993) 496–503.

[6] Agarwal, G.S., Bhuptawat, H. K. and Chaudhari, S., "Biosorption of aqueous chromium (VI) by Tamarindus indica seeds," Bioresour. Technol., 97(2006) 949-956.

[7] Chen, J.P. and Wang, X.Y., "Removing copper, zinc, and lead ion by granular activated carbon in pretreated fixed-bed columns," Sep. Purif. Technol., 19, (2000)157–167.

[8] Jeme, E.A., "Controls of manganese, iron, cobalt, nickel, copper and zinc concentrations in soils and water," Adv. Chem. Ser., 7, (1968) 33-37.

[9] Thomas, M.J. and Theis, T.L., "Effects of selected ions on the removal of chrome hydroxide," J. Water Pollut. Control Fed., 48, (1976) 20-32.

[10] Dean, J.G., et al.," Removing heavy metals from waste water," Environ. Sci. Technol., 6 -518(1972).

[11] Inove, Y. and Munemori, M., "Co-

precipitation of Hg(II) with Fe(III) hydroxide," Environ. Sci. Technol., 1, (1968)34-43.

[12] Rouse, J.U., "Removal of heavy metals from industrial effluents," J. Eng. Div., 102 (EE5), (1976) 929.

[13] Netzer, A. and Wilkinson, P., "Removal of heavy metals from wastewater by adsorption on sand," in Proceedings of the 29th Industrial Waste Conference, vol. 29, Purdue, p. 841 (1974).

[14] Grote, M. and Kittrup, A., "Enrichment and extraction of heavy metal ions from water by means of selective chelate-forming ion-exchange resins," GIT Fachz Lab., 23 -393(1979).

[15] Bin, Y., "Adsorption of copper and lead from industrial wastewater by maple sawdust," Thesis, Lamar University (1995).

[16] Aguwa, A.A., "Sorption of cadmium ions from dilute aqueous solutions by chelate ion-exchange resins," ME Thesis, Howard University, Washing-ton, DC (1981).

[17] Arthur, I. and vogel, D., Sc. (Lond.), D.I.C., F.R.I.C, "A Text-Book of Quantitative Inorganic Analysis Including Elementary Instrumental Analysis," 791-792(1998).

[18] Lagergren, S., "About the theory of so-called adsorption of soluble substance," Kung. Sven. Veten. Hand., 24, (1898) 1–39.

[19] Ofomaja, A.E.," Sorptive removal of methylene blue from aqueous solution using palm kernel fibre: effect of fibre dose," Biochem. Eng. J. 40 (1), (2008) 8–18.

[20] Aharoni, C. and Sparks, D.L.," Kinetics of soil chemical reactions: a theoretical treatment," in: D.L. Sparks, D.L. Su´arez (Eds.), Rates of Soil Chemical Processes, Soil Science Society of America, Madison, Wisconsin, (1991) pp. 1–18.

[21] Chen, D. Z., Zhang, J. X. and Chen, J. M.," Adsorption of methyl tert-butyl ether using granular activated carbon: Equilibrium and kinetic analysis," Int. J. Environ. Sci. Tech., 7 (2), (2010) 235-242.